Composite connections between CFS beams and plywood panels for flooring systems: Testing and Analysis

Dheeraj Karki[1]; Suleiman Al-Hunaity[2]; Harry Far[3]; Ali Saleh[4]

Abstract:

A composite floor consisting of cold-formed steel (CFS) beams connected to structural plywood panels is a sustainable and economical alternative to concrete only floors or the traditional floor systems supported by solid lumber joists. The structural performance of the composite CFS-plywood floor depends on the strength and stiffness properties of the shear connection. In this study, an experimental investigation into the load-slip behaviour of connections between CFS and plywood panels constructed with self-drilling screws, coach screws, and nut and bolt is presented. The influence of structural adhesives at the shear interface alongside fasteners is also investigated. The stiffness, ductility and load-carrying capacity of the eight different types of connections were evaluated through a series of push-out tests. Nut and bolt connections demonstrated to be the best choice as a shear connector followed by self-drilling screws. However the size of the nut and bolt to be determined based on the crushing strength of timber itself. Connection with coach screws only demonstrated to be less stiff and relatively low ductile than other tested shear connections. Composite connections with fasteners alongside with adhesives demonstrated higher stiffness and load-capacity than the fastener alone. Furthermore, a simple analytical expression for the load-slip response of the connections is proposed based on the Foschi formula, which showed a good correlation with test results. Based on all the observations made, self-drilling screws and M8 nut and bolts are recommended to be used as shear connectors for lightweight composite cold-fromed steel and timber flooring system.

Keywords: *Cold-Formed Steel Joists; Structural plywood; Shear connection; Push-out tests; Load-slip behaviour*

1PhD Candidate in School of Civil and Environmental Engineering, Faculty of Engineering and Information Technology, University of Technology Sydney (UTS), Building 11, Level 11, Broadway, Ultimo, NSW 2007 (PO Box 123), Sydney, Australia (Corresponding author) Email: Dheeraj.karki@student.uts.edu.au

2PhD Candidate in School of Civil and Environmental Engineering, Faculty of Engineering and Information Technology, University of Technology Sydney (UTS),Sydney, Australia, Email: Suleiman.AlHunaity@uts.edu.au

3Senior Lecturer in Structural Engineering, School of Civil and Environmental Engineering, Faculty of Engineering and Information Technology, University of Technology Sydney (UTS),Sydney, Australia, Email: Harry.Far@uts.edu.au

4Senior Lecturer in Structural Engineering, School of Civil and Environmental Engineering, Faculty of Engineering and Information Technology, University of Technology Sydney (UTS),Sydney, Australia, Email: Ali.Saleh@uts.edu.au

1 INTRODUCTION

Lightweight flooring systems consisting of cold-formed steel joists and different timber floorboards are used for the construction of residential floors and the mezzanine floors in the commercial and industrial building because they have a high strength to weight ratio and provide economical and durable solutions (Kyvelou et al., 2017; Parnell et al., 2010; Karki and Far, 2021). The benefit of composite construction in hot rolled steel and concrete (Ellobody and Young, 2006; Rackham et al., 2009; Mirza and Uy, 2009), timber and concrete (Deam et al., 2008; Khorsandnia et al., 2016; Lukaszewska et al., 2010) are well established with minimal studies on the structural performance of cold-formed steel and timber floors (Kyvelou et al., 2017, 2018; Zhou et al., 2019). Consequently, the beneficial interaction between cold-formed steel joists and timber floorboards is mostly unsubstantiated resulting in conservative designs. Xu and Tangorra (2007) and Parnell et al. (2010) carried out experimental studies into the vibration behaviour of cold-formed steel and timber-based floor systems but did not consider the influence of composite action within serviceability performance of such floors.

The role of shear connectors for the efficient design of hot-rolled steel and timber flooring systems has been demonstrated through a series of push-out tests on connection joints (Hassanieh et al., 2017a, 2016b) and four-point bending tests on a large scale steel-timber composite beams (Hassanieh et al., 2016a; Loss and Davison, 2017). Moreover, Hassanieh et al. (2017b) suggested that the structural behaviour of a steel-timber composite system is significantly influenced by stiffness and load-carrying capacity of connections. Studies have been carried out on the use of cold-formed steel sections with concrete as an alternative

solution to replace hot-rolled steel and reinforced concrete (Hanaor, 2000; Bamaga et al., 2019). The strength and stiffness of the composite beam rely mainly on the shear interaction. Cold-formed steels are thin-walled, so the practice of using headed stud to the top flange of steel beam as in traditional composite system is not applicable to cold-formed steel composite beams (Hanaor, 2000; Lakkavalli and Liu, 2006). Hence, attention should be given to the selection and design of shear connections in cold-formed steel floors.

Li et al. (2012) examined the potential of lightweight bamboo and cold-formed steel composite slab through full-scale testing and highlighted the importance of shear connection to the stiffness of the composite system. Recent experimental studies (Kyvelou et al., 2017; Zhou et al., 2019), which utilised self-drilling screws as a means of shear connection, demonstrated the benefits of composite action on the moment capacity and flexural stiffness of the composite cold-formed steel and timber flooring system. Numerical studies (Karki et al., 2021; Far, 2020) into the structural behaviour of composite cold-formed steel and timber flooring system also demonstrated the beneficial effect of composite action on the load-carrying capacity of the composite beams. More recently, experimental analysis (Vella et al., 2020) into cold-formed steel to timber connections with inclined screws was carried out by conducting push-out tests. It was found that inclined screws at 45^{o} resulted in higher stiffness than 0^{o} screws. Although the findings from these investigations on cold-formed steel and timber composite system look promising, those studies seem to be focused on screws only as shear connectors. Furthermore, there is a necessity to develop and investigate different shear connectors with higher stiffness and ductility to enhance the composite efficiency and load-carrying capacity of cold-formed steel and timber flooring systems.

Nowadays, the prefabricated building construction method is gaining popularity and has reduced environmental impacts during construction and provided cost and material effective houses while decreasing the construction time (Navaratnam et al., 2021; Navaratnam et al., 2019). Cold-formed steel and engineered timber products make the right choice in prefabricated construction industries as they are sustainable and lightweight. Modular units like cold-formed steel and timber composite floors can be fabricated off-site and joined on-site. Hence, it is crucial to understand the behaviour of connections used to join timber panels to the cold-formed steel joists. A series of material tests and push-out tests were conducted to determine the mechanical properties of the employed materials and response of shear connections as a part of experimental investigation.

In this paper, the performance of the CFS-plywood composite connection is experimentally investigated. The means of shear connections adopted in this study were mechanical fasteners alone and adhesives and mechanical fasteners. The use of mechanical fasteners with adhesives is to investigate the composite performance of the system in comparison to the one with mechanical fixings only. Kyvelou et al. (2017) reported the significant influence of structural adhesive on the moment capacity and flexural stiffness of the cold-formed steel and timber composite floor. As the results from the studies seem promising, it has become apparent to further study the influence and behaviour of structural adhesive along with mechanical fixings to a further extent. Hence, this study investigates the short-term load-slip response, ultimate load carrying capacity, stiffness, and failure mode of CFS-plywood composite connections by conducting push-out tests. Lastly, by carrying out the non-linear

regression analysis of the experimental results, empirical formulae for the load-slip response of the CFS-plywood connections are proposed.

2 EXPERIMENTAL PROGRAM

2.1 Push-out specimens

Laboratory push-out tests on eight major groups of CFS-plywood connections have been performed, and each group consist of three identical specimens. Hence, a total number of twenty-four push-out specimens were fabricated and tested. The push-out specimens utilised 2.4mm thick CFS C-section with 45mm thick structural plywood panels. The cross-sectional dimension of the CFS joist used in the push-out tests is shown in Fig. 1.

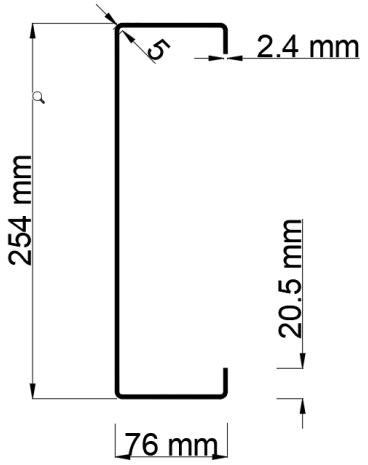

Fig. 1. Cross-section dimensions of CFS C-section used in the test

The details of the push-out specimens are given in Table 1. In Table 1, the test series identification system adopted is a letter 'P', which indicates a push-out test, followed by connection types. For example, the label 'P-SDS' indicates a push-out test series that uses

self-drilling screws as shear connectors. Similarly, any test series that utilised structural adhesive on the CFS flange and plywood interface used a letter 'a' at the end. For instance, 'P-CSa' indicates a push-out test series that used coach screws and adhesives as a means of shear connection.

Table 1. Summary of push-out specimen details

Test series	Type of connection	Number of specimen tested
P-SDS	#14 Self-drilling screw	3
P-SDSa	#14Self-drilling screw + adhesive	3
P-CS	M12 Coach screw	3
P-CSa	M12 Coach screw + adhesive	3
P-NB12	M12 Nut and bolt (without washer)	3
P-NB12a	M12 Nut and bolt (without washer)+ adhesive	3
P-NBW12	M12 Nut and bolt (with washer)	3
P-NBW8	M8 nut and bolt (with washer)	3
		24

The geometry and set-up adopted for the tests are shown in Fig.2. The symmetric setup was adopted to ensure an even distribution of loading. To fabricate an economical size of the test specimens, 200 mm shear connector spacing was chosen, which is half of the construction industry practice. It is also worth mentioning that full-scale bending tests of the cold-formed steel and plywood flooring will be done with 200 mm and 400 mm connector spacing. Hence the load-slip behaviour of the shear connection from this study is crucial for future numerical studies.

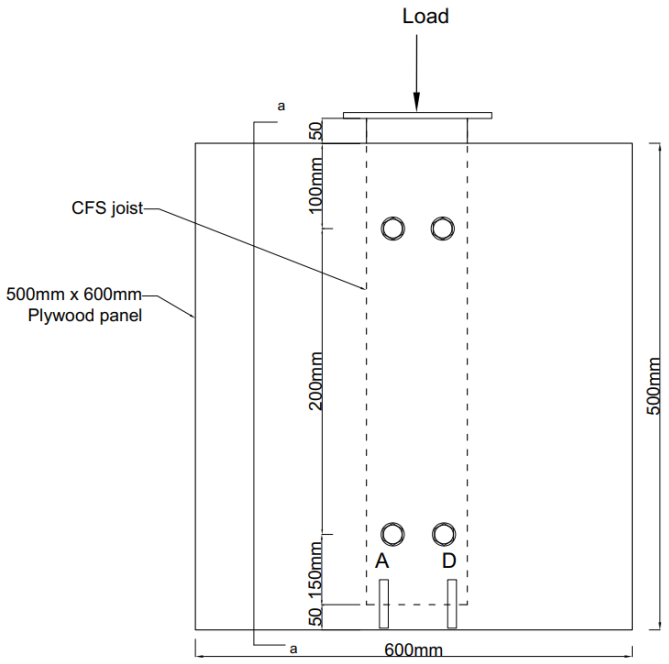

(a)

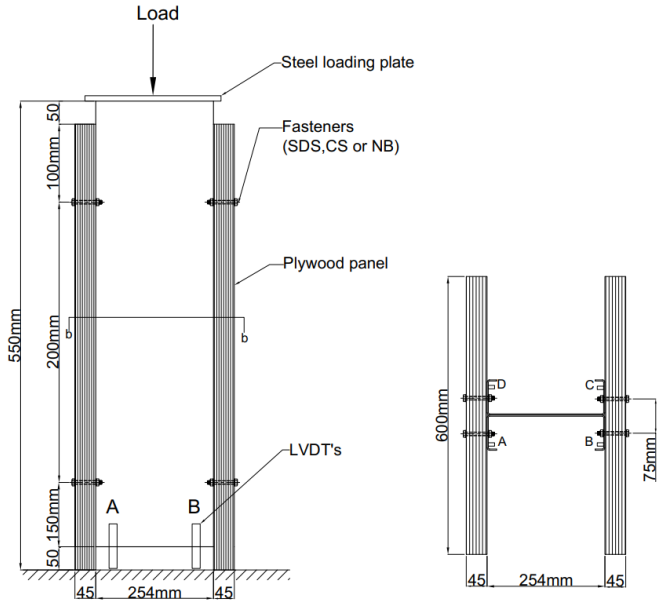

(b) (c)

Fig. 2. Push-out specimen schematic view: (a) Elevation view; (b) Section view a-a ; (c) Plan view b-b

The primary variables considered in the experimental program were four different types of mechanical fasteners (e.g., self-drilling screws, M12 coach screws, M8 nut and bolt, M12 nut and bolt), and the use of structural adhesive along with fasteners. The effect of washers on the strength and stiffness of specimens with M12 nut and bolt connectors is also investigated.

2.2 **Material properties**

2.2.1 *Structural plywood*

The structural plywood panels were F11 stress graded made from Radiata Pine supplied by Big River Group Pty Ltd. The thickness of the plywood panel was 45mm. Samples obtained from the plywood panels were utilised to carry out bending, compressive and tensile tests. Four specimens were tested for each tests. The tests were conducted as per AS/NZS 2269.1:2012 (Standard Australia, 2012) to determine the material properties of the plywood panels. The average measured strength and stiffness properties of the plywood panels are provided in Table 2. The load-displacement curve obtained from four-point bending tests for parallel and perpendicular samples is shown in Fig. 3. The gradient of the load-deflection curve from Fig. 3 is an important parameter for the calculation of modulus of elasticity.

Table 2. Average measured mechanical properties of structural plywood (in MPa)

Bending parallel to grain ($f_{b,0}$)	Bending perpendicular to grain ($f_{b,90}$)	Tension parallel to grain ($f_{t,0}$)	Tension perpendicular to grain ($f_{t,90}$)	Compression parallel to grain ($f_{c,0}$)	Compression perpendicular to grain ($f_{c,90}$)	Modulus of Elasticity (E)
40	45.5	22	17	31.5	28	10000

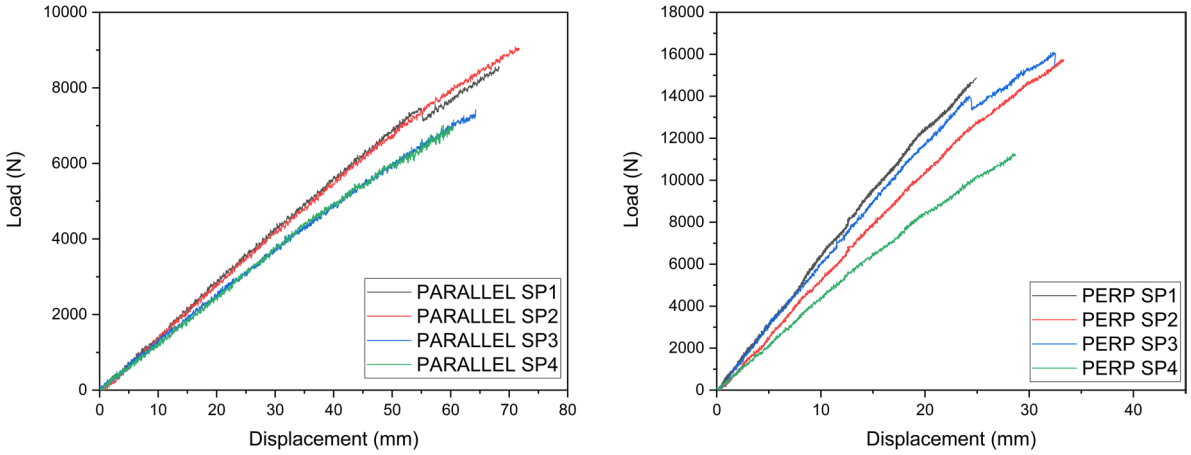

(a) (b)

Fig. 3. Load-displacement curve obtained from bending test of plywood (a) Parallel specimens (b) Perpendicular specimens

2.2.2 *Cold-formed steel*

Coupons extracted from the cold-formed steel joist were undertaken for tensile tests to determine the material characteristics of the joist. A total of eight tensile coupons were tested of which four were extracted from web and four were extracted from the flange of the CFS joist. The tests were conducted as per AS 1391:2007 (Standard Australia, 2007). The stress-strain curve obtained from the tensile tests for all the specimens is given in Fig. 4. The average measured mechanical and geometrical properties of the CFS joist are provided in Table 3.

Table 3. Mechanical and geometrical properties of CFS beam

Thickness, t (mm)	Height,h (mm)	Flange width,bf (mm)	Elastic modulus (MPa)	Yield strength (MPa)	Tensile strength (MPa)
2.4	254	76	207000	504	567

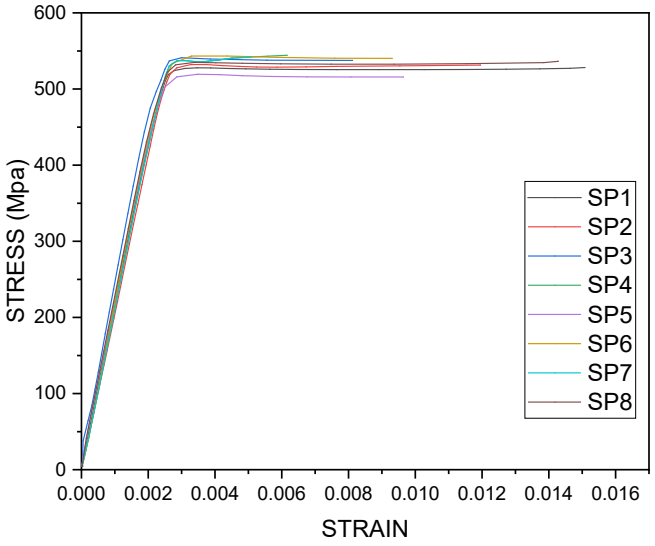

Fig. 4. Stress-strain curve obtained from tensile tests

2.2.3 *Mechanical fasteners*

Size 14 self-drilling screws (6mm diameter), coach screws (Size M12), nut and bolt (Size M8 and M12) were used in the testing as a means of shear connections. Coach screws and nuts and bolts were made of Grade 4.6 steel with nominal yield and ultimate strength of 240 MPa and 400 Mpa. Self-drilling screws, coach screws and bolts comply with the requirements of AS3566.1(Standard Australia, 2002), AS1393(Standard Australia, 1996), and AS1110.1(Standard Australia, 2000), respectively. The outline of fasteners used in the push-out tests is shown in Fig.5.

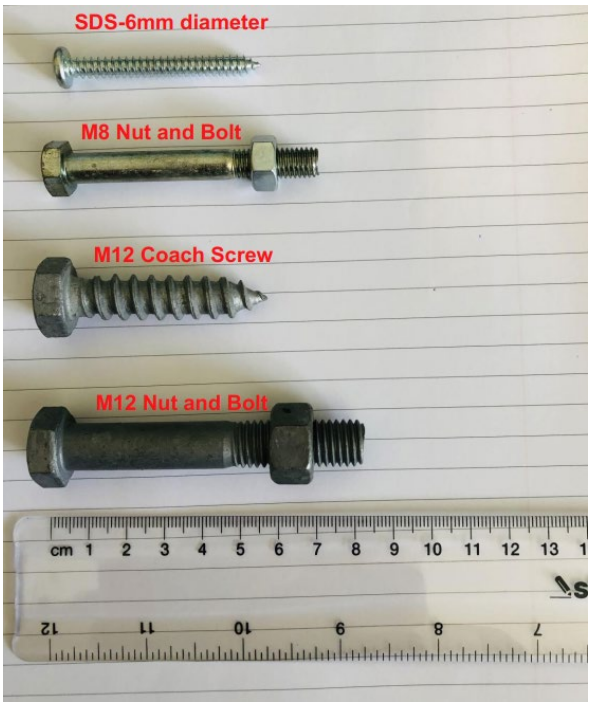

Fig. 5. Shear connectors used in push-out tests

2.2.4 *Structural adhesives*

Structural adhesive (SikaBond-Contactfix) was used in the interface between cold-formed steel and plywood along with the mechanical fasteners in three of the test series shown in Table 1. The mechanical properties of the adhesive as per the manufacturer are provided in Table 4.

Table 4. Mechanical properties of structural adhesive

Tensile strength (MPa)	Compressive strength(MPa)	Shear strength (MPa)	Coefficient of linear expansion
30	70	15	$60x10^{-6}$ mm^{o}c

2.3 **Test setup and fabrication**

The push-out tests configuration might impact the test results due to the uneven load distribution on the specimen caused by mono-symmetric section geometry of CFS joists. Therefore, to guarantee a stable configuration, two CFS joists were joined back to back, and two plywood panels were connected on both sides of the flange, as illustrated in Fig. 1.

After cutting the plywood panels to a required size, which is 500 mm × 600 mm, both the panels and the flange of the CFS C-section were pre-drilled except for the specimens with the self-drilling screws. The diameter of the pre-drilled holes in the plywood panels was 1 to 1.5 mm smaller than the diameter of the coach screws and 0.5 to 1 mm larger than the diameter of the bolts. The diameter of the pre-drilled holes in the flange of the C-section was 0.2mm to 0.6mm larger than the connectors (coach screws and bolts). The bolts were tightened using a manual torque wrench. The structural adhesive or glue was applied on both the CFS flange and plywood panel surface for the glued specimens. After mounting the plywood panel and CFS C-section together, the specimen was left to dry the glue for 24 hours before installing the screws or bolts.

The overall experimental setup is shown in Fig. 6. All the tests were conducted using a 300 kN capacity Shimadzu universal testing machine. The relative displacement or slip between the CFS beam and plywood panels was measured using four LVDTs (linear variable differential transformers) with a 50 mm stroke. Four 60×6×6 mm steel brackets were fixed to the flange of the CFS joist, and the LVDTs were fixed to the plywood panels. The LVDTs were in approximate level with contact in steel bracket, so the relative slip between plywood panel and joist was measured when the load was applied on the CFS joist.

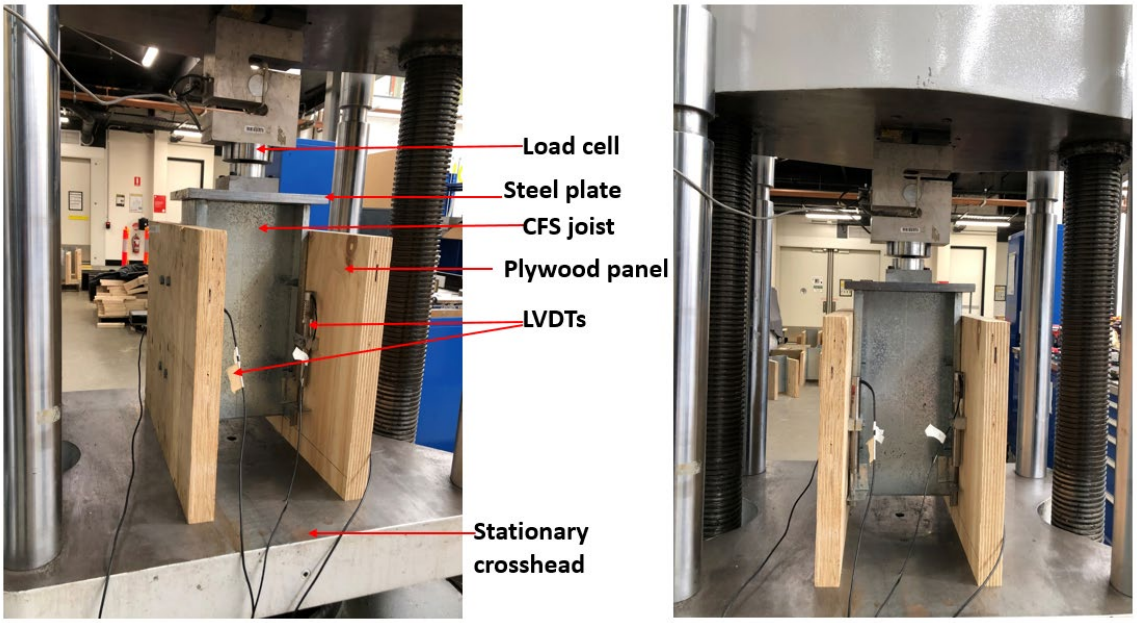

Fig. 6. Experimental setup for push-out test in Shimadzu universal testing machine

2.4 **Load application**

All of the specimens were loaded according to the instructions given in BS EN 26891:1991(British Standard, 1991). Fig. 7 shows the loading technique in line with the standard.

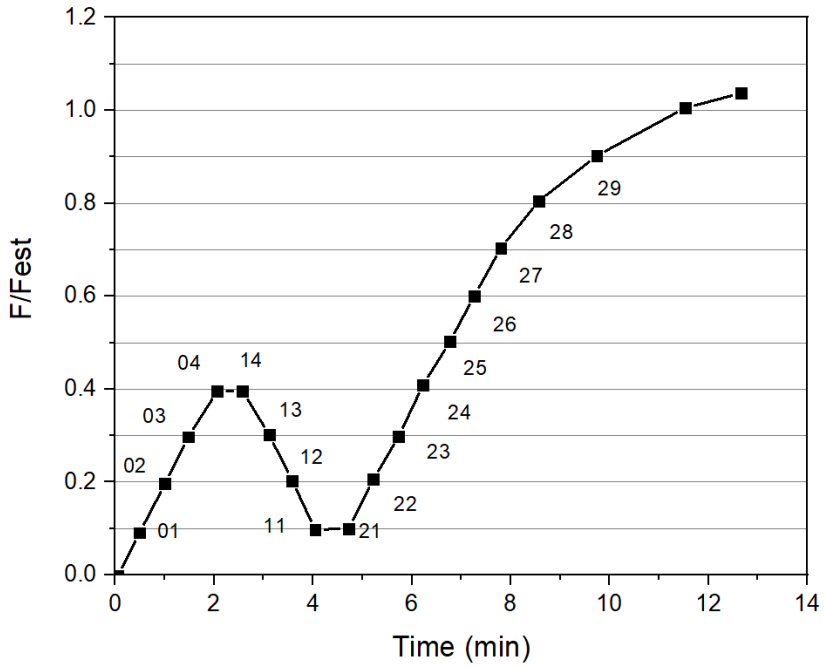

Fig. 7. Loading procedure adopted in push-out tests as per BS EN 26891

A preliminary test was conducted from each series to determine the ultimate load, F_u. F_u is the load that corresponds to the failure of a specimen due to the connection failure or a 15 mm slip recorded during the test. Based on F_u (ultimate load) from the preliminary test, F_{est} (estimated failure load) was obtained. F_{est} is necessary for loading, unloading and reloading cycles as per the standard. The load was initially increased from 0 to $0.4F_{est}$ and was maintained at $0.4F_{est}$ for 30 s. Afterwards, the specimen was unloaded from $0.4F_{est}$ to $0.1F_{est}$, and the load was sustained for 30 s at $0.1F_{est}$. Finally, a constant load rate was applied up to $0.7F_{est}$, and a constant rate of slip was applied above $0.7F_{est}$ until the specimen failed. The displacement rate for the self-drilling screw specimen was 1mm/min, whereas the displacement rate for the coach screw, nut, and bolt specimen was 2mm/min to make the specimens fail within 3-5 minutes. All the specimens failed at about 11 to 15 minutes, which aligns with the total testing time specified in the standard.

3 DISCUSSION OF TEST RESULTS

Hassanieh et al. (2016b) reported that the structural behaviour of timber connections could be affected by the mechanical properties of materials and the method of fabrication. Hence, three identical specimens for each type of CFS-plywood joint (Fig. 2 and Table 1) were fabricated and tested under similar loading conditions to ensure the accuracy and repeatability of the test results (e.g., stiffness, failure mode, and load-slip response). This section presents the distinct failure modes of the specimens and their load-slip responses from each test series.

3.1 Modes of failure

3.1.1 *Connections with self-drilling screws*

Fig. 8 demonstrates the failure mechanism of the specimens with SDS connection joint. The body of the screw was effectively restrained by the plywood preventing any rotation, and the head was under the flange of the CFS joist. As the loading was applied through the steel plate on CFS joists, the body of the screw was pressed into the plywood, and the region of the screw under the head at the CFS-plywood interface started to yield in bending. Upon further loading, the head of the screw detached from its body. All the specimens failed due to shear failure under the head of the screws. The bending of the screws was also observed, as shown in Fig. 9.

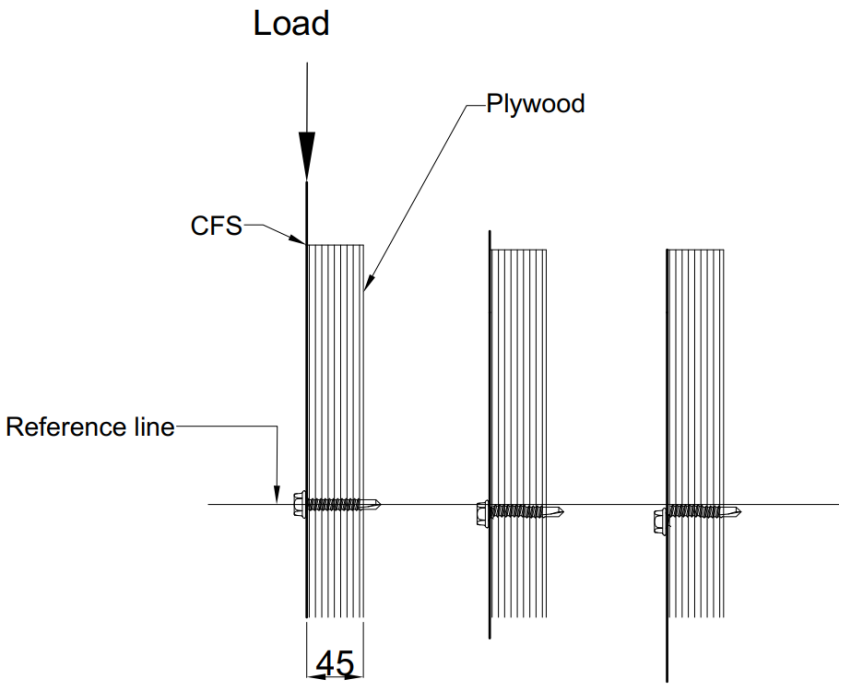

Fig. 8. Failure mechanism of the specimens with self-drilling screws

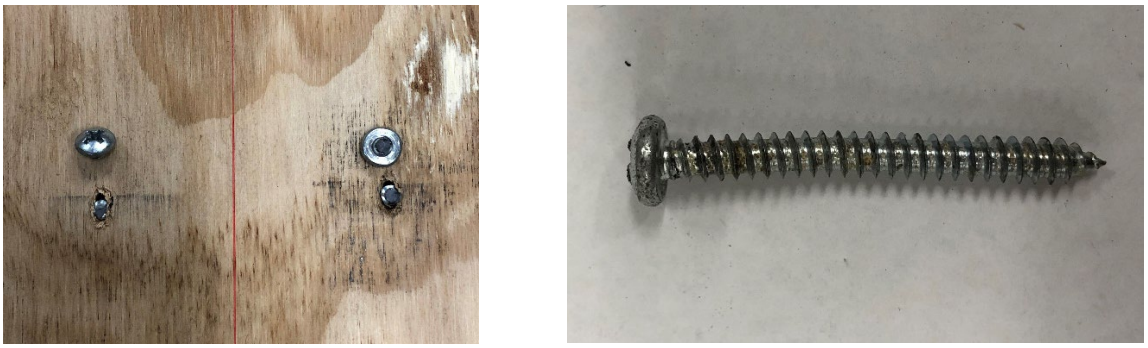

(a) (b)

Fig. 9. Failure modes of the specimens with self-drilling screws: (a) shear failure under head; (b) bending failure

3.1.2 *Connections with coach screws*

The failure mode of the push-out specimens with coach screw connections is shown in Fig. 10.

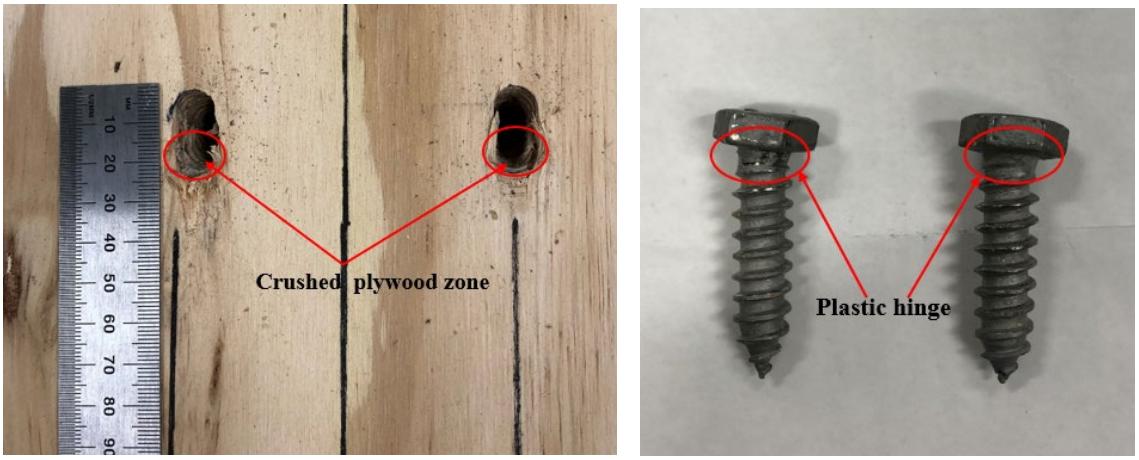

(a) (b)

Fig. 10. Failure modes of the specimens with coach screws: (a) crushing of plywood; (b) formation of plastic hinge

Formation of plastic hinge occurred under the head of the coach screw almost on every fastener. When the push-out specimens were loaded, coach screws gradually rotated with the head moving towards the loading direction while the body was pressed into the plywood. The plywood panel was sufficient enough to restrain the bodily displacement of the coach screw even though significant bearing of the coach screw into the plywood was observed. The crushing of the plywood panels was observed, which were almost double the size of the coach screw. A simplified failure mechanism of the specimens with CS connection joint is demonstrated in Fig. 11.

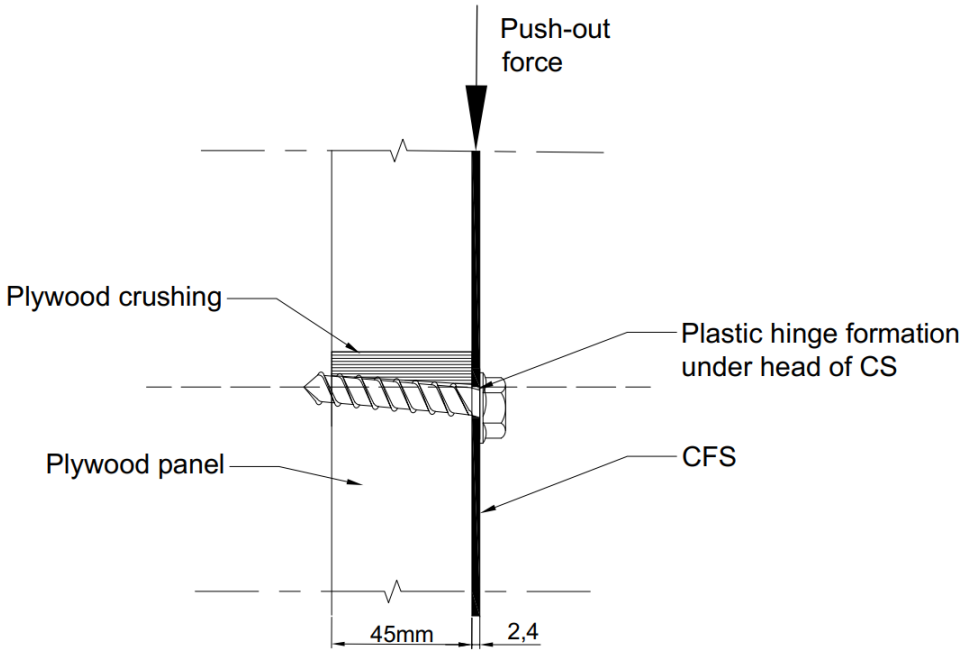

Fig. 11. Failure mechanism of the specimens with coach screws

3.1.3 *Connections with M12 nut and bolt (without washer)*

The typical failure mode for the specimens with M12 nut and bolt (without washer) connections were the formation of plastic hinge and crushing of plywood panels, as shown in Fig. 12. When the push-out specimens were loaded, the load was perpendicular to the longitudinal axis of the bolt. With the gradual movement of the CFS joist due to the loading, plastic hinge formation took place near the threaded part of the bolt, which lies at the shear interface of plywood and CFS joist. Because the unthreaded body part of the bolt was restrained by the plywood panels and the threaded part being moved slowly along the loading direction subtle plastic hinge formed at the shear interface. The illustration of the failure mechanism of this connection type is shown in Fig. 13. As mentioned earlier, the failure

criteria for all the tested specimens was taken as 15 mm joint slip as per BS EN 26891; loading was stopped at around 15 to 17 mm slip. The extent of the plywood crushed zone was double the size of the fastener, as observed in the coach screw connection.

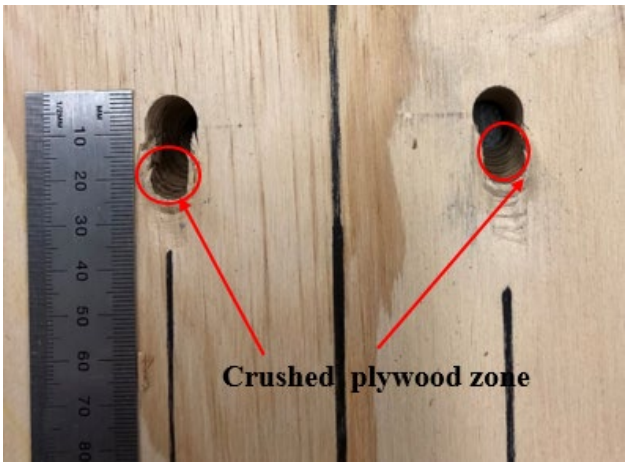

(a)

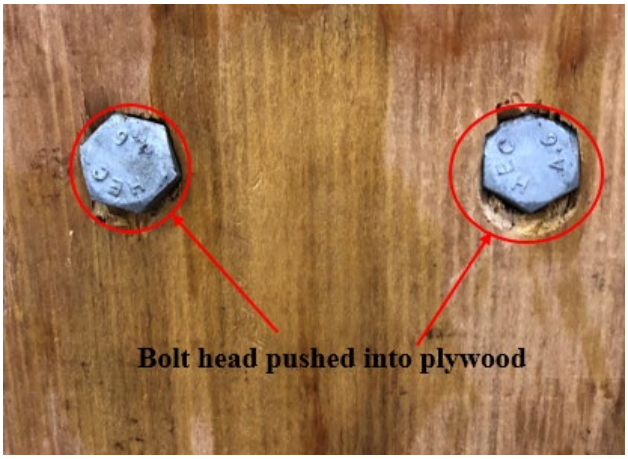

(b)

(b)

Fig. 12. Failure modes of the specimens with M12 nut and bolts: (a) crushing of plywood; (b) bolt head bearing into plywood; (c) plastic hinge

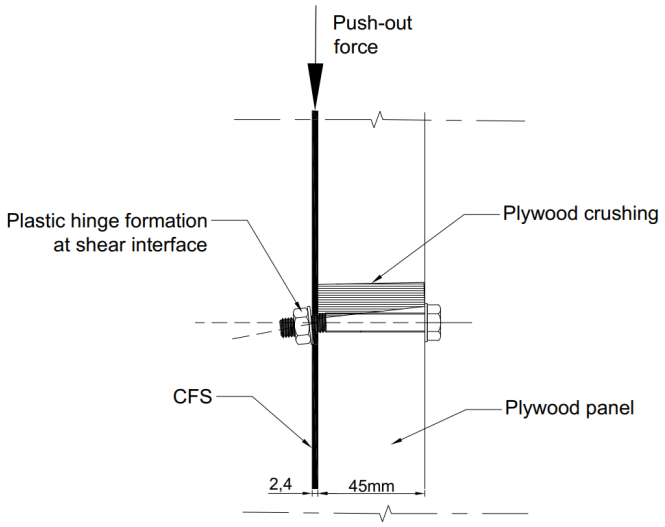

Fig. 13. Failure mechanism of the specimens with M12 nut and bolt (without washer)

3.1.4 *Connections with M12 nut and bolt (with washer)*

The distinctive failure mode of the specimens with M12 nut and bolt with washer (P-NBW12) is shown in Fig. 14. Two plastic hinges formed on the connector, one at the middle part (similar to the connections with M12 nut and bolt without washer) and the other near the bolt head. The crushing of plywood panels was similar to that of the P-NB12 test series specimen. With the increasing load on the push-out specimen, the bolt end on the CFS joist side gradually displaces in the direction of load, and the unthreaded part restrained by plywood panels got pressed into the plywood. Hence because of that phenomenon, a permanent deformation in the plywood panels, which hadthe size of washers, was observed, as shown in Fig. 14(c). Local deformation around the fastener holes of the CFS joist was also found in these connection joints.

(a)

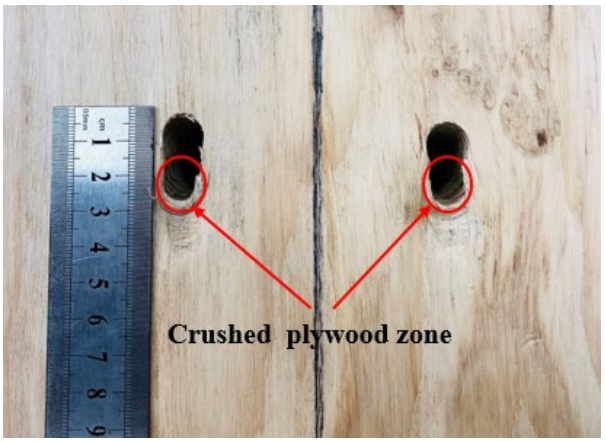

(b)

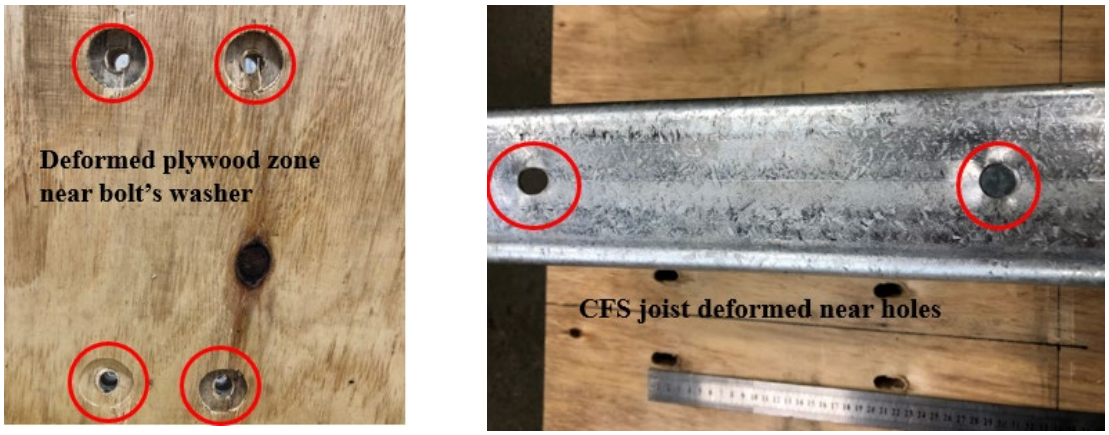

(c) (d)

Fig. 14. Failure modes of the specimens with M12 nut and bolts (with washers): (a) plastic hinge formation; (b) crushing of plywood; (c) washer at bolt head pressed into plywood; (d) local deformation of CFS joist flange around holes

3.1.5 *Connections with M8 nut and bolt (with washer)*

Fig. 15 shows the typical failure modes associated with the M8 nut and bolt connections. All the specimens on the test series P-NBW8 demonstrated the formation of a plastic hinge on the bolt and, ultimately, its fracture. At the initial loading stage, all the specimens were within the elastic range, and the slip of the connection joints showed a linear relationship with the loading. With the increasing load, bending of the bolts and formation of plastic hinge took place near the threaded part of the bolt, which lies at the shear interface of plywood and CFS joist. As the load was further increased, some connectors could not bear more loads and ultimately failed in the shear plane. The failure of these shear connectors was more of a brittle nature, while the coach screws and M12 nut and bolt demonstrated semi-ductile or ductile of its kind.

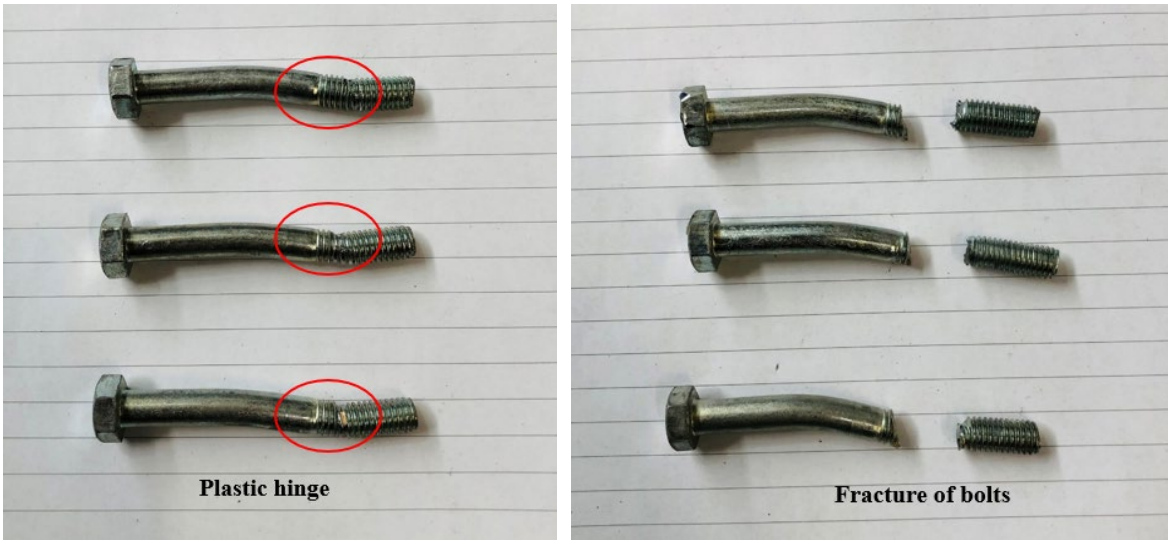

(a) (b)

Fig. 15. Failure modes of the specimens with M8 nut and bolts (with washers): (a) plastic hinge formation; (b) fracture of bolts

3.1.6 *Connections with structural adhesive+fasteners (self-drilling screw, coach screw or nut and bolt)*

As can be seen in Table 1, three different test series: P-SDSa, P-CSa, and P-NB12a that utilised self-drilling screws, M12 coach screws, and M12 nut and bolt, respectively, along with structural adhesives were tested. There was a sudden failure of the adhesives on the specimens with SDS and CS, meaning that debonding occurred at one point with the increasing load. This phenomenon was not observed for the nut and bolt connections. However, it should be noted that the failure mode of the specimens with and without adhesives was pretty much similar, which are already discussed in the above sections. Fig. 16 shows the failure modes associated with fasteners and adhesives connection.

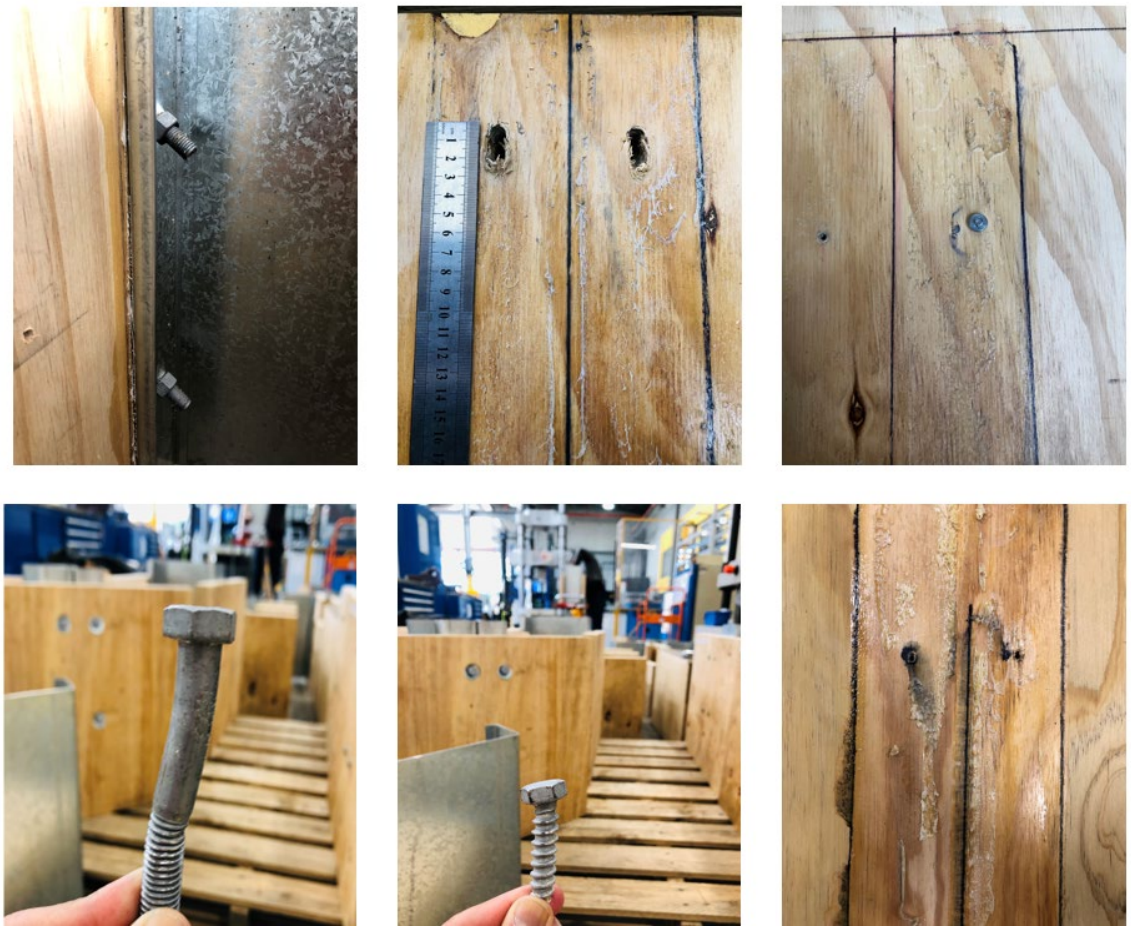

Fig. 16. Failure modes of the specimens with fasteners + adhesives

3.2 **Load-slip response of connection joints**

When a composite CFS and timber beam assembly is loaded, the load is transferred from the timber sheathing through the shear connectors into the CFS beams beneath the sheathing. It is well known that the amount of load that can be shared depends on the amount of slip that arises between two members. This slip value also known as slip modulus helps to understand the extent of composite action that takes place in the assembly (Couchman, 2016). The load-slip responses of each connection types is discussed in this section. It should be noted that,

joint slip of 15 mm is considered as the failure of connections throughout the push-out tests. This is one of the failure criteria as outlined in BS EN 26891. And also the reason to record failure load at 15 mm slip rather than going up to the ultimate load of connectors (especially M12 nut and bolts) is that usually at around 15 mm slip, bearing of fastener into the plywood and crushing of plywood panel would have significantly taken place, even though the connection itself was taking higher load. Hence adopting 15 mm joint slip as a failure criteria was reasonable, considering the strength properties of materials tested.

3.2.1 *Connections with self-drilling screws only (Test series: P-SDS)*

The load-slip behaviour of the connections with 6mm diameter self-drilling screws is shown in Fig. 17. The load-carrying capacity P_u and stiffness $K_{0.4}$ and $K_{0.6}$ of the connections are provided in Table 5. The slip stiffness values $K_{0.4}$ and $K_{0.6}$ are the corresponding values at 40% and 60% of the peak load, respectively and are considered initial and pre-peak stiffness of the connections. The slip modulus values $K_{0.4}$ and $K_{0.6}$ are calculated using the procedures given in BS EN 26891. It was found that the initial stiffness of the connections was higher than the pre-peak stiffness. In all specimens, a sudden drop in the load was observed once there was breakage of the screw head.

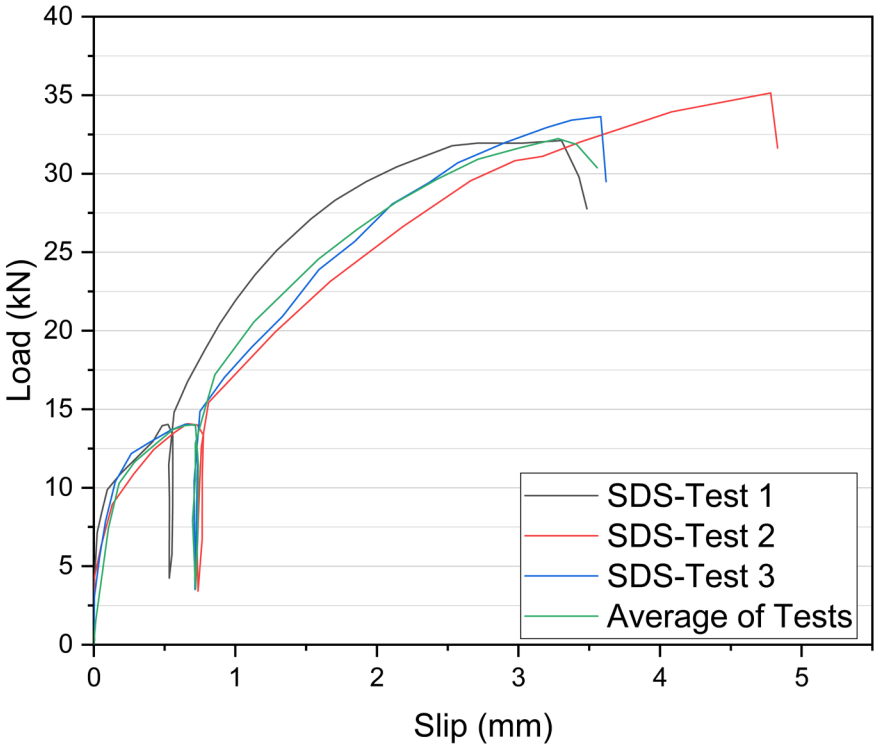

Fig. 17. Load slip response of specimens with self-drilling screws (SDS)

Table 5. Load-carrying capacity and slip modulus of self-drilling screw

Self-drilling screw (SDS)	Load at failure, P_u (kN)	$K_{s,\,0.4}$ (kN/mm)	$K_{s,\,0.6}$ (kN/mm)
Test 1	32.2	22.1	20
Test 2	35.1	15.93	14.8
Test 3	33.6	17.63	14.92
Average of tests	32.26	17.59	16.99

3.2.2 *Connections with coach screws (Test series: P-CS)*

Table 6 summarises the test results of the connection joints with M12 coach screw connectors. Furthermore, the load-slip response of the connection is depicted in Fig. 18.

Table 6. Load-carrying capacity and slip modulus of coach screw

Coach screw (CS)	Load at failure, P_u (kN)	$K_{s,\,0.4}$ (kN/mm)	$K_{s,\,0.6}$ (kN/mm)
Test 1	81.98	11.39	11.32
Test 2	82	10.63	10.6
Test 3	84.5	11.38	11.4
Average of tests	82.8	10.89	10.66

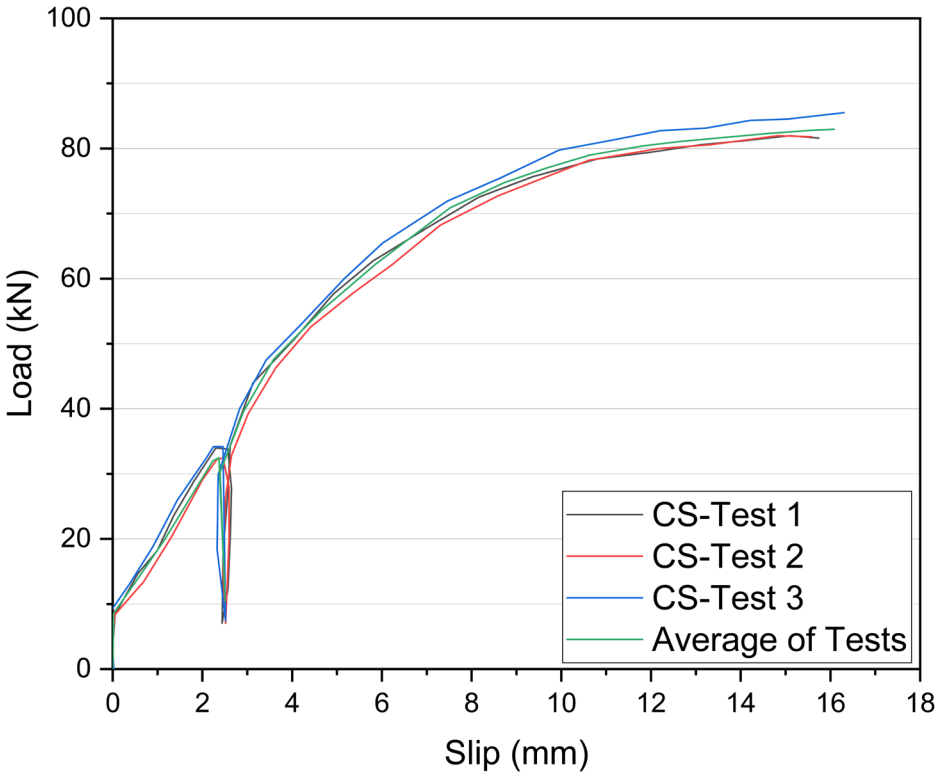

Fig. 18. Load slip response of specimens with coach screws (CS)

The initial stiffness ($K_{0.4}$) and the pre-peak stiffness ($K_{0.6}$) of these connection types were nearly similar. Unlike in SDS connections, which do not require pre-drilling, CS connections were pre-drilled both in plywood panels and CFS joists. It could be the reason to have nearly similar stiffness as there was no pre-tension or post-tension force to increase the friction between the material while loading.

3.2.3 *Connections with M12 nut and bolts (Test series: P-NB12 and P-NBW12)*

The load-slip response of the CFS and plywood connections using M12 nut and bolt connectors without and with washers is shown in Fig. 19 and 20, respectively.

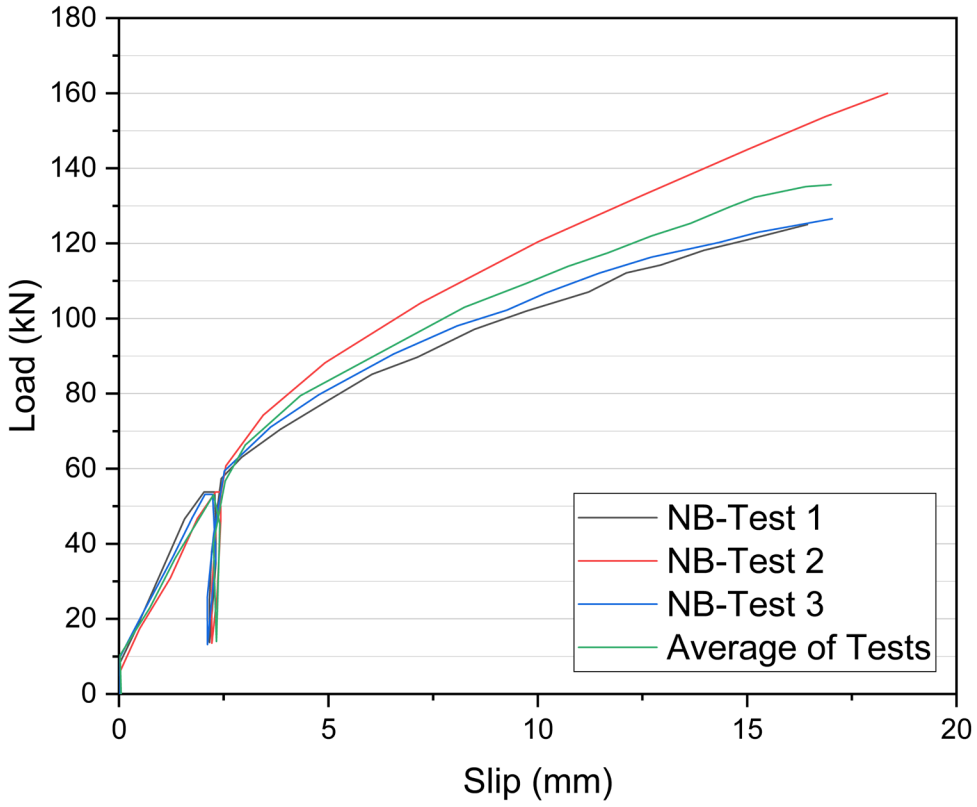

Fig. 19. Load slip response of specimens with M12 nut and bolt without washer (NB12)

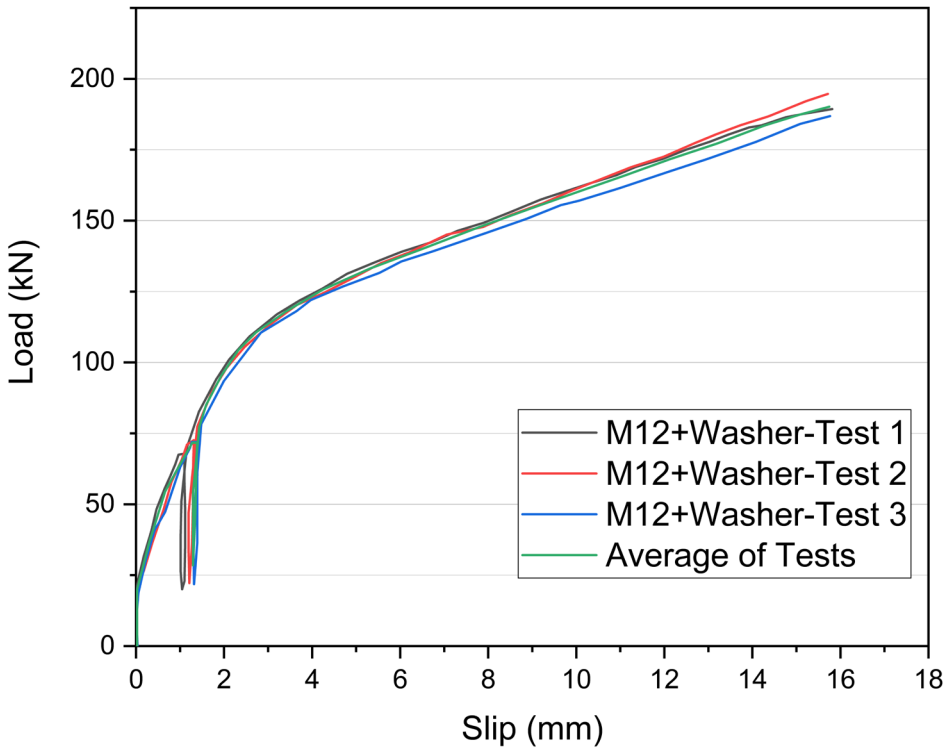

Fig. 20. Load slip response of specimens with M12 nut and bolt with washer (NBW12)

The initial stage, which is also the no-slip stage, was due to the pre-tensioning of bolts. Bolt pretensioning leads to the significant friction between the plywood panel and CFS joist and hence negligible relative slip at the shear interface.With the increasing load, slip started to increase proportionally up to 60% of the loading for the connectors without washers. While for the connectors with washers, the slip was relatively lower with increased loading. The load-slip behaviour was non-linear until 6 mm joint slip for the connections with the washer. As expected, connections that used nut and bolt with washer demonstrated higher stiffness than without washer. The load-carrying capacity P_u, stiffness $K_{0.4}$, and $K_{0.6}$ of the connections without and with washer are provided in Tables 7 and 8, respectively.

Table 7. Load-carrying capacity and slip modulus of M12 nut and bolt (without washer)

Nut and bolt (NB)	Load at failure, P_u (kN)	$K_{s,\ 0.4}$ (kN/mm)	$K_{s,\ 0.6}$ (kN/mm)
Test 1	121	22.91	16.5
Test 2	145	22.18	20.6
Test 3	123	21.85	17.2
Average of tests	132	21.96	18.26

Table 8. Load-carrying capacity and slip modulus of M12 nut and bolt (with washer)

Nut and bolt (NB)	Load at failure, P_u (kN)	$K_{s,\ 0.4}$ (kN/mm)	$K_{s,\ 0.6}$ (kN/mm)
Test 1	186.5	51.4	40
Test 2	188	46.95	38.94
Test 3	180	44.77	36.14
Average of tests	183.5	44.4	36.8

3.2.4 *Connections with M8 nut and bolt (Test series: P-NBW8)*

Fig. 21 depicts the load-slip curves for specimens that used M8 nuts and bolts with washers. There was a very minimal slip until the load reached 4 kN, and this initial resistance was due to the tightness of the composite joints as a result of the pre-tensioning of bolts. Almost all the specimens failed due to fracture of bolts, and hence a sudden drop in the load can be seen in Fig. 21. The key values measured from the testing of three identical specimens are presented in Table 9. The fracture of bolts as shown in Fig. 15(b) is consistent with the sudden drop of load in the curve below a 15 mm slip value.

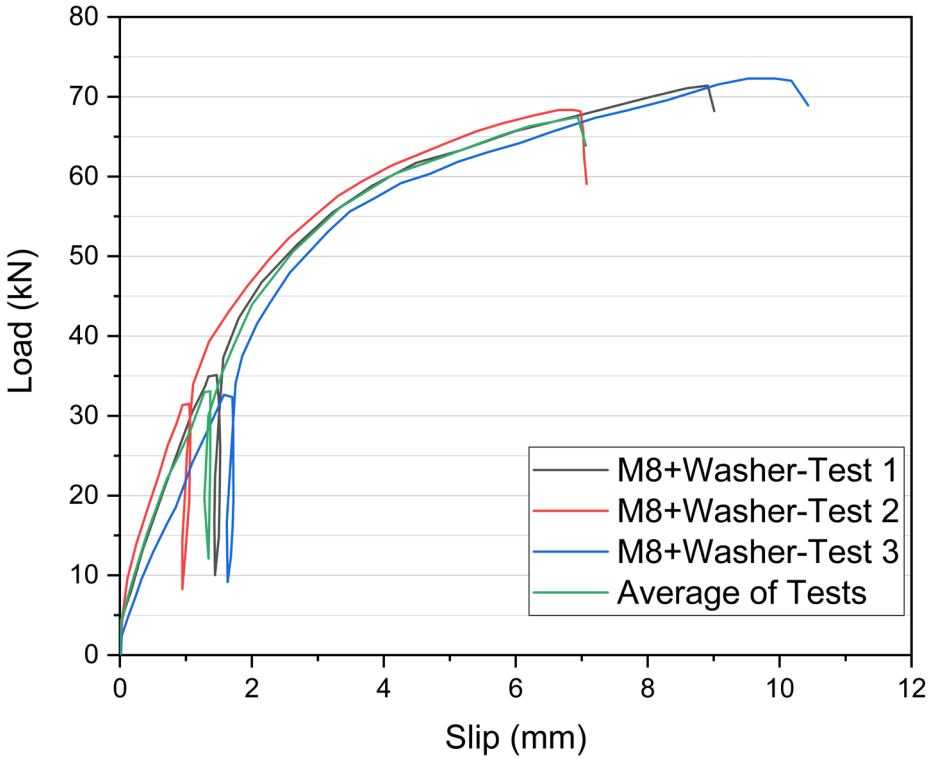

Fig. 21. Load slip response of specimens with M18 nut and bolt with washer (NBW8)

Table 9. Load-carrying capacity and slip modulus of M8 nut and bolt (with washer)

Nut and bolt (NB)	Load at failure, P_u (kN)	$K_{s,\,0.4}$ (kN/mm)	$K_{s,\,0.6}$ (kN/mm)
Test 1	71.4	23.7	23.3
Test 2	68.2	26.7	22.35
Test 3	72	18.35	19.95
Average of tests	67.6	20.2	20

3.2.5 *Connections with fasteners + adhesives (Test series: P-SDSa, P-CSa, and P-NB12a)*

The purpose of using adhesives at the shear interface of plywood and CFS joist with fasteners was to increase the composite behaviour so that the connection joints behaved as full composite sections with no slip. Furthermore, with the use of structural adhesive/glue, the initial stiffness of the connections was found to be significantly increased. There was no slip

until 5 kN load for the specimens with SDS and glue and 9 kN load for the specimens with CS and glue. But the minimal slip was recorded for the specimens with nut and bolt and glue. The load versus slip response of the test series P-SDSa, P-CSa, and P-NB12a is shown in Fig. 22, Fig. 23, and Fig. 24, respectively.

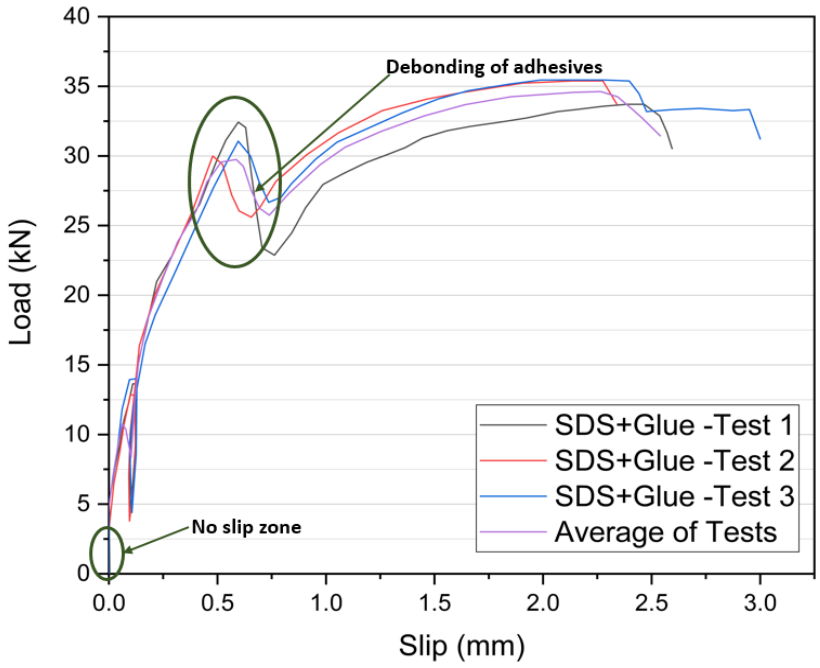

Fig. 22. Load slip response of specimens with SDS + Glue

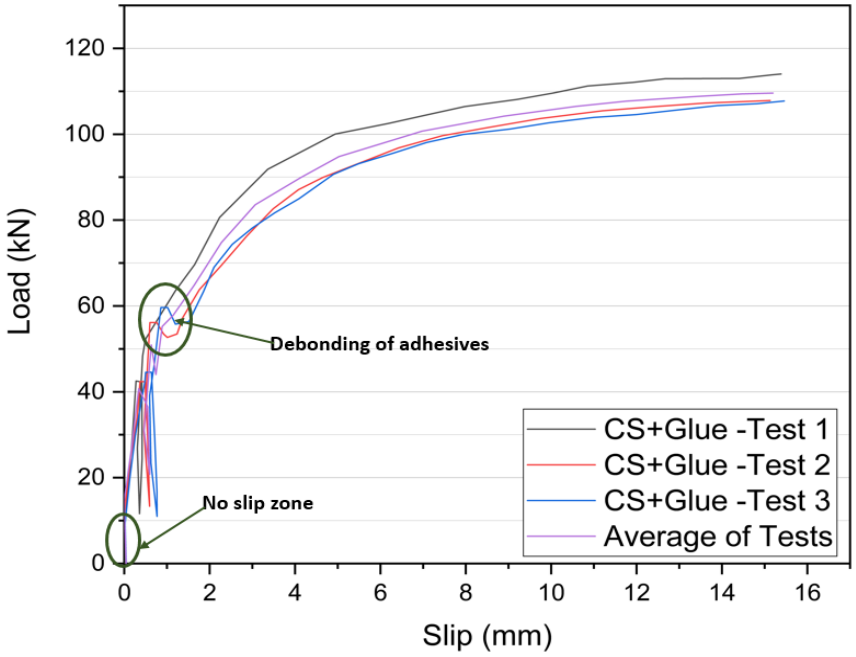

Fig. 23. Load slip response of specimens with CS + Glue

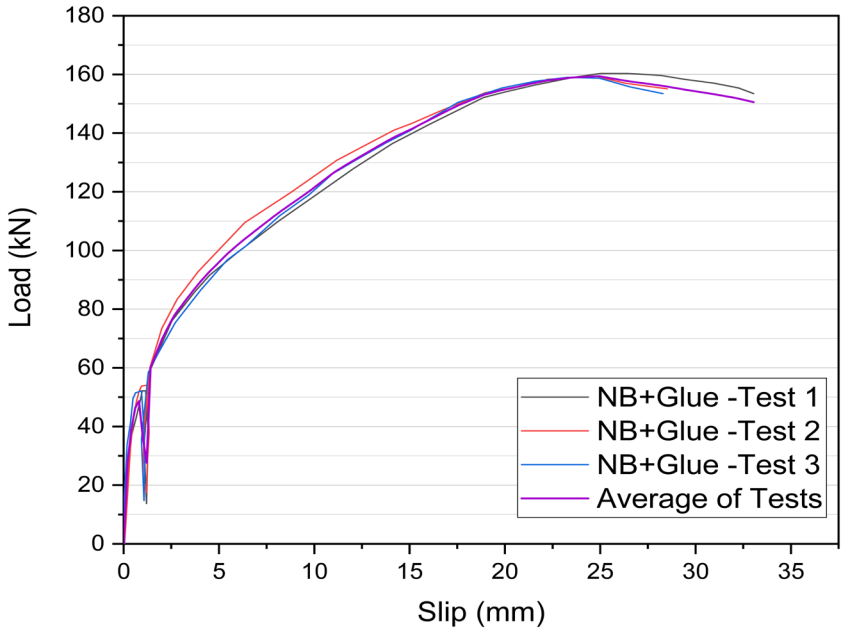

Fig. 24. Load slip response of specimens with NB + Glue

A sudden drop in the load after 40% of the loading was observed for the test series P-SDSa, and P-CSa which was due to the delamination of the glue from the shear interface and resulted in brittle failure. But no such phenomenon was observed in the P-NB12 test series. After this brief process of glue failure, the specimens started to take higher loads which can be attributed to the fact that the strength of composite joints relied on the fastener alone. The summary of the test results for P-SDSa, P-CSa, and P-NB12a are provided in Tables 10, 11, and 12, respectively.

Table 10. Load-carrying capacity and slip modulus of SDS + Glue (Test series P-SDSa)

SDS + Glue	Load at failure, P_u (kN)	$K_{s,\ 0.4}$ (kN/mm)	$K_{s,\ 0.6}$ (kN/mm)
Test 1	33.7	84	84.1
Test 2	35.3	90.5	83.1
Test 3	35	82	68
Average of tests	34.6	90.5	73.7

Table 11. Load-carrying capacity and slip modulus of CS + Glue (Test series P-CSa)

CS + Glue	Load at failure, P_u (kN)	$K_{s,\ 0.4}$ (kN/mm)	$K_{s,\ 0.6}$ (kN/mm)
Test 1	113	60.4	39.25
Test 2	107.2	52.2	25.4
Test 3	106.7	48.6	24.3
Average of tests	110	52	29.4

Table 12. Load-carrying capacity and slip modulus of M12 NB + Glue (Test series P-NB12a)

NB + Glue	Load at failure, P_u (kN)	$K_{s,\ 0.4}$ (kN/mm)	$K_{s,\ 0.6}$ (kN/mm)
Test 1	137.5	45.2	26.4
Test 2	142.4	47.67	30.4

Test 3	141	70.46	30.16
Average of tests	140.8	55.7	31.5

3.3 **Overview of test findings**

As shown in Table 1, eight test series and each test series with three identical specimens were tested. In the above sections, the load-slip behaviour and failure mode of individual tests were discussed. An average of tests was also calculated for each test series as shown in Fig. 17 to Fig. 24, and Table 5 to Table 12 by running a mathematical analysis in a graphing and analysing tool called Origin Pro (OriginPro, 2021). However, a distinctive comparative summary of the results obtained from all the test series is presented in this section. Table 13 summarises the key results obtained from all the push-out test series regarding their mean values.

Table 13. Summary of key test results (mean values) for different shear connections

Test series	Load at failure, P_u (kN)	$K_{s,\ 0.4}$ (kN/mm)	$K_{s,\ 0.6}$ (kN/mm)	Ductility, D	Normalised stiffness $K_{s,\ 0.4}$ (kN/mm)	Normalised stiffness $K_{s,\ 0.6}$ (kN/mm)
P-SDS	32.2	17.59	16.99	4.8	2.19	2.12
P-SDSa	34.6	90.5	73.7	23.4	11.31	9.21
P-CS	82.8	10.89	10.66	5.3	1.36	1.33
P-CSa	110	52	29.4	15.7	6.5	3.6
P-NB12	132	21.96	18.26	7.1	2.75	2.28
P-NB12a	140.8	55.7	31.5	19	6.96	3.93
P-NBW12	183.5	44.4	36.8	11.2	5.55	4.6
P-NBW8	67.6	20.2	20	6.1	2.52	2.5

The slip modulus at 40% (initial stiffness) and 60% (pre-peak stiffness) of the loading is calculated per shear connector, which is the normalised stiffness as tabulated in Table 13. The ductility of the connections, which is the ability to undergo large slip without reducing strength, is also determined by Equation (1) in accordance with BS EN 12512 (CEN, 2005).

$$D = \frac{V_u}{V_y} \quad (1)$$

Where V_u and V_y are the ultimate slips and yield slips, respectively, as defined in BS EN 12512. It was found that the use of structural adhesives along with fasteners significantly increased the stiffness and ductility of the connections. Test series, P-SDSa, which utilise self-drilling screws and adhesive at the shear interface between two materials, produced stiffer and more ductile connections than any other test series. There was no pre-drilling required for the specimens that use SDS. Even though SDS is smaller in diameter and lesser in strength than CS and bolts, the threads of the screws firmly clamped with CFS flange and plywood after drilling, which produced post-tensioning force. As a result, very high friction exists between CFS and plywood panels due to the influence of glue and post-tensioning force. Hence, the composite joints act as a perfect composite section with minimal slip and higher stiffness. Connection joints with CS only (P-CS) were demonstrated to be less stiff and relatively low ductile than others. However, with the use of adhesive at the shear interface along with CS (P-CSa), the ductility and average stiffness of the connections were increased by 196% and 255%, respectively. Similarly, for the M12 nut and bolt connections, the use of adhesives enhanced the stiffness by 270% and ductility by 167%. Comparing the specimens, P-NB12 and P-NBW12, the stiffness and ductility were found to be increased by 100% and 58%, respectively, for M12 nut and bolt connections with washers. The stiffness

and ductility of M12 nut and bolt connection without washers (P-NB12) were 9% and 16% higher than the connections with M8 nut and bolt with washer (P-NBW8). The reason here is, with the use of washers, more pre-tension force was applied on the bolts with lesser local damage on the plywood itself. Higher pre-tension force, which was developed while tightening the bolts, created a compressive force on the connection joints, which ultimately increased the rigidity of the joints.

4 ANALYTICAL LOAD-SLIP MODEL OF CONNECTIONS

In this section, a non-linear regression analysis on the load-slip behaviour of the tested connection joints is carried out to develop an analytical relationship of load versus slip. An equation developed by Foschi (Foschi, 1977) is used in this study to predict the load slip relationship of the connections. A slight modification of the Foschi formula is made in this study to capture the no-slip response and non-linear behaviour of the connection joints. Foschi formula is widely used to simulate the load-slip relationship of the mechanical connections like nails, bolts (Kalkert and Dolan, 1997; Yang et al., 2020). The expression for the Foschi curve is given by Equation (2).

$$P(s) = (P_O + K_1.S).\left(1 - e^{\left(\frac{-k_O.S}{P_O}\right)}\right) \quad (2)$$

A four-parameter model based on the Foschi formula is used in this study to predict the load-slip relationship, which is given by Equation (3).

$$P(s) = P_i + (P_{max} - P_i).\left(1 - e^{\left(\frac{-k_o.S}{Po}\right)}\right) \quad (3)$$

Where $P(s)$ is the load for a slip S (mm), K_o (kN/mm) is the initial stiffness of connection, K_1 (kN/mm) is the stiffness for large slip values, P_i (kN) is the intercept of asymptote with slope K_o, P_o (kN) is the intercept of asymptote with the slope K_1, P_{max} (kN) is the maximum load recorded for the failure of the test. These parameters are obtained by the non-linear curve fitting of the experimental test results, as shown in Fig. 25. In Fig. 25, P_i and P_o are the intercept of the asymptote on y-axis before and after yield respectively. P_i corresponds to an initial load after no-slip and P_o corresponds 50% to 60% of the failure load. Origin pro software (OriginPro, 2021) was used for the non-linear regression based on the exponential CDF to determine input parameter values.

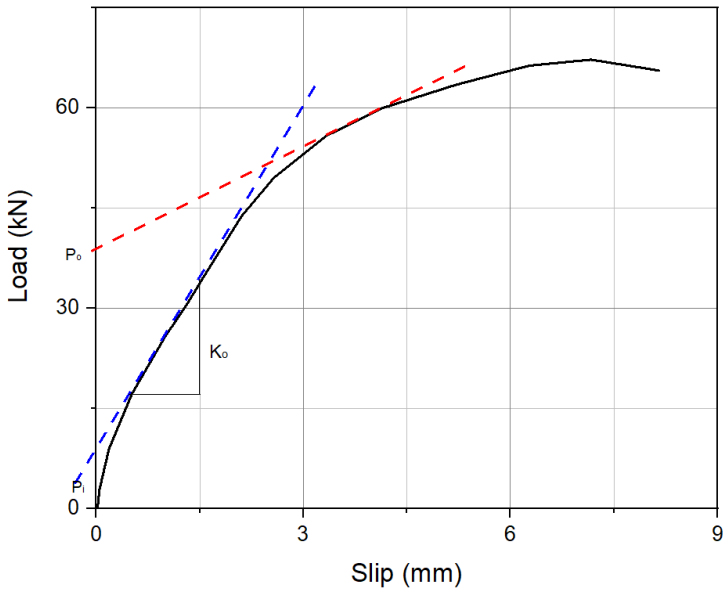

Fig. 25. Stiffness parameters for load slip behaviour for modified Foschi formula

The calculated parameters from the average results of all the test series are presented in Table 14, and the predicted load-slip graphs using the modified Foschi formula are shown in Fig.

26. As can be seen, the load-slip curves from the analytical equation has a good correlation with the mean of experimental results. The analytical prediction was capable of predicting the initial response and the non-linear behaviour after yielding of the experimental load-slip curves. In table 14, P(s) from the modified Foschi curve is calculated as per Equation (3) and compared with corresponding P(s) values obtained from the tests. The accuracy of the predicted formula is more clearly seen from the comparison of actual failure load and predicted ultimate/failure load values. R-square values for the modified Foschi curve are also provided in Table 14. The values are greater than 0.91, meaning the predicted curves are more than 91% accurate, which demonstrates a close agreement between the curve fit models and experimental results.

Table 14. Key parameters of modified Foschi formula for the tested CFS and plywood connections

Test series	P_i (kN)	P_o (kN)	$P_{max} - P_i$ (kN)	K_0 (kN/mm)	P(s) test (kN)	P(s) formula (kN)	R^2
P-SDS	0	15	36	8.4	32.2	30.9	0.91
P-SDSa	2.4	22	30.4	80	34.6	32.8	0.95
P-CS	0	42.5	82	10	82.8	79.5	0.95
P-CSa	13	38	91	18	110	104	0.95
P-NB12	7	90	132	16	132	129	0.91
P-NB12a	10	110	145	19	140.8	144	0.93
P-NBW12	16	114	165	26	183.5	175	0.95
P-NBW8	2	30	65.9	9.5	67.6	65.2	0.93

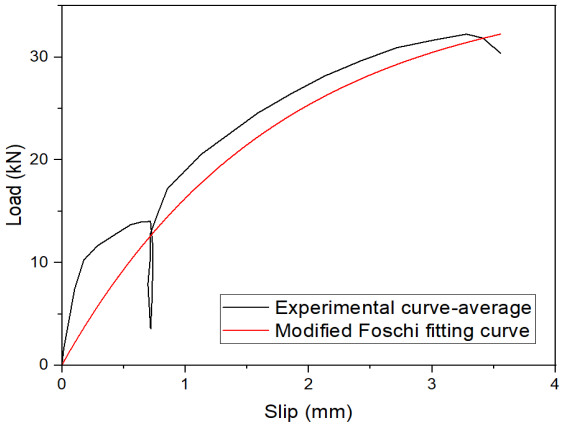

(a) Test series P-SDS

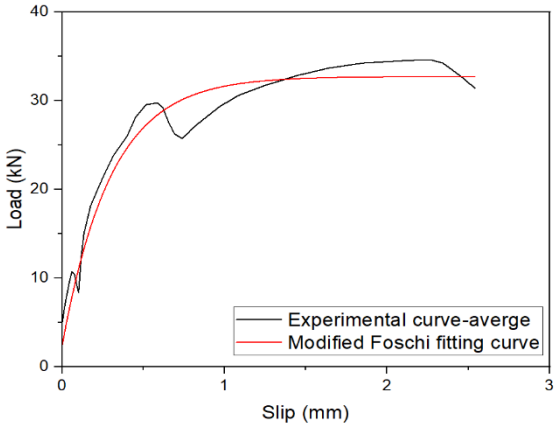

(b) Test series P-SDSa

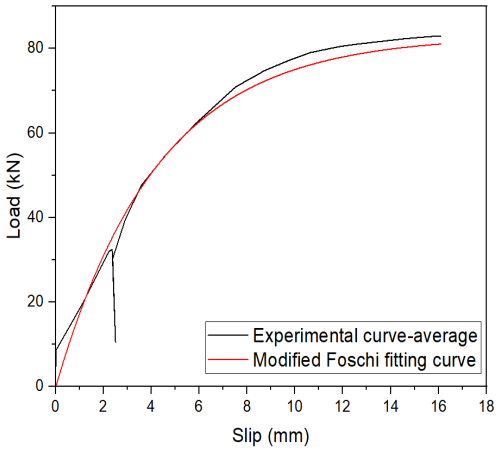

(c)Test series P-CS

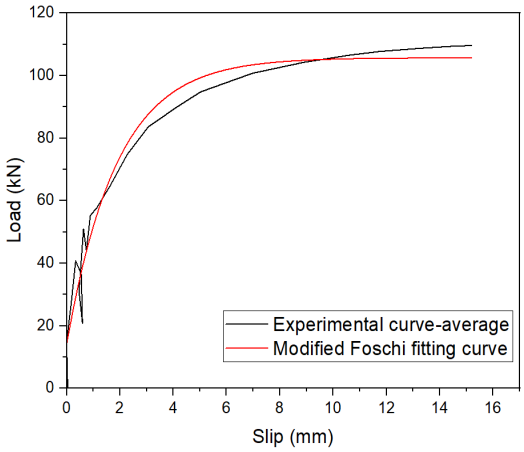

(d)Test series P-CSa

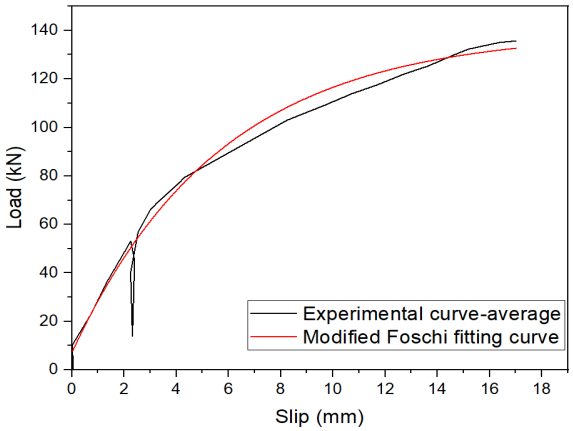

(e) Test series P-NB12

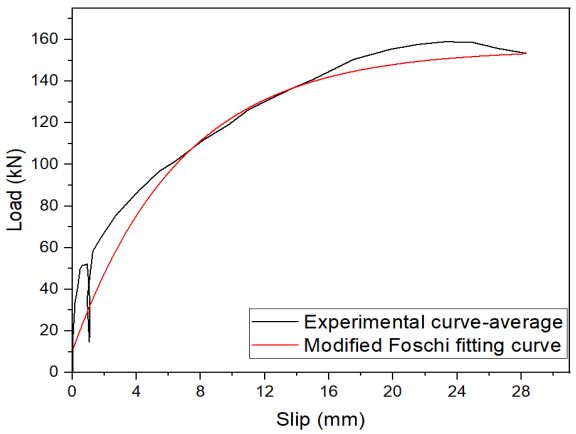

(f) Test series P-NB12a

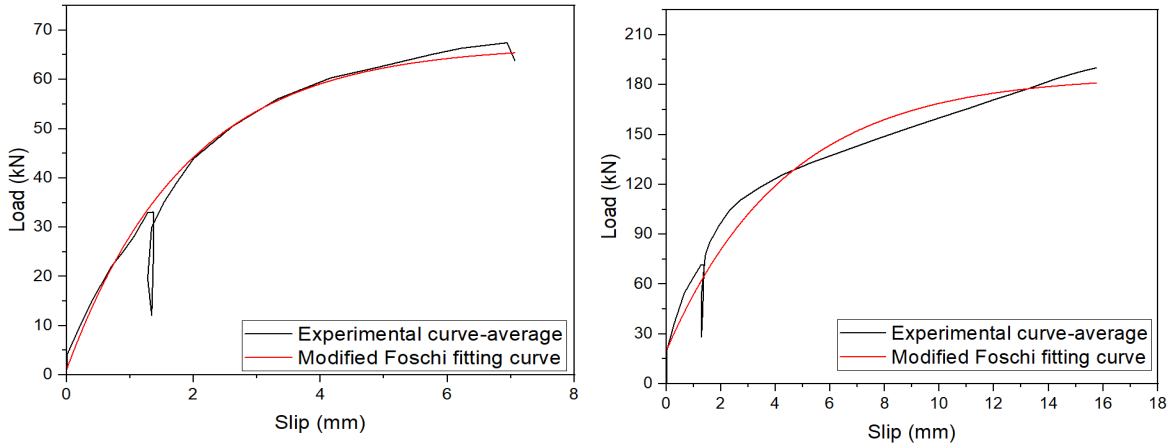

(g) Test series P-NBW8 (h) Test series P-NBW12

Fig. 26. Comparison between analytical model and mean of experimental load-slip curves for CFS and plywood composite connections

5 CONCLUSIONS

The ductility and stiffness of shear connection plays a crucial role in the load-carrying capacity of composite floors. As a results, static push-out tests on CFS and plywood connections were carried out on a total of 24 specimens in this study. The load-slip behaviour and failure mode of CFS and plywood composite connections on eight different connection types are investigated and evaluated. The effect of different fastener types (Self-drilling screw, coach screw, nut and bolt with and without washer) with and without structural adhesives were investigated in terms of their load-slip response and ductility. As expected, composite connections with fasteners alongside adhesives performed better than the fastener alone. Among them, self-drilling screws with adhesive at the interface of the CFS joist and plywood panel (Test series: P-SDSa) demonstrated the highest serviceability, ultimate stiffness, and ductility. However, the load-carrying capacity of these connections was much lower than other connection types. In terms of the connection without adhesives, M12 nut and bolt with washers (Test series: P-NBW12) had superior ductility and stiffness, among

others. The load-carrying capacity of these connections was also higher than any other connection type. It was seen that the use of washers with the bolts helped to take higher pre-tension force, which ultimately helped to improve the strength and stiffness of the fastener. M8 nut and bolt with washer (Test series: P-NBW8) and M12 nuts and bolts without washers (Test series: P-NB12) had similar results in terms of stiffness and ductility. The stiffness and ductility of M12 coach screw connections (Test series: P-CS) were the lowest among other connections, but the load-carrying capacity was higher than SDS and adhesive connections. And lastly, an analytical equation was formulated based on the Foschi formula to predict the load-slip behaviour of the tested connections. The load-slip curves obtained from the analytical formula were in good agreement with the response obtained from the physical tests.

For the construction of lightweight composite flooring systems using cold-formed steel and plywood, fasteners play a vital role in an efficient and economical design. The design of such flooring systems is governed by the ultimate limit state and serviceability limit state requirements. Just because large mechanical fasteners like M12 have higher stiffness and ductility doesn't mean they are the best choice as shear connections for composite CFS and plywood flooring systems. From the push-out tests carried out in this study, it was observed that the structural behaviour of the CFS-plywood joints with large mechanical fasteners (e.g. M12 nut and bolt, M12 coach screw) is primarily governed by the behaviour of plywood panels (e.g. plywood crushing) rather than the strength and stiffness of fasteners. Hence based on the observation made on push-out test results, self-drilling screws and M8 nut and bolts would make an ideal fit as mechanical fasteners for designing composite cold-formed steel

and timber flooring systems. And the use of structural adhesives along with fasteners can enhance the strength and stiffness of the system.

Future investigations including bending tests on large scale composite CFS and plywood beams will be carried out in the near future by the authors to study and quantify the benefits of composite action using the shear connections discussed in this paper.

Acknowledgements

The authors are grateful to Peter Brown at UTS Tech Lab for providing technical assistance throughout the testing.

Data Availabiltiy Statement

No data, models, or code were generated or used during the study.

References

Bamaga, S., Tahir, M. & Shek, P. N. 2019. Structural Behaviour of Cold-Formed Steel of Double C-Lipped Channel Sections Integrated with Concrete Slabs as Composite Beams. *Latin American Journal of Solids and Structures,* 16.

British Standard 1991. BS EN 26891:1991 Timber structures-Joints made with mechanical fasteners.

Cen 2005. BS EN 12512 Timber structures-Test methods-Cyclic testing of joints made with mechanical fasteners. European Committee for Standardization.

Couchman, G. H. 2016. Minimum degree of shear connection rules for UK construction to Eurocode 4. Steel Construction Institute.

Deam, B. L., Fragiacomo, M. & Buchanan, A. H. 2008. Connections for composite concrete slab and LVL flooring systems. *Material and Structures,* 41**,** 495-507.

Ellobody, E. & Young, B. 2006. Performance of shear connection in composite beams with profiled steel sheeting. *Journal of Constructional Steel Research,* 62**,** 682-694.

Far, H. 2020. Flexural Behavior of Cold-Formed Steel-Timber Composite Flooring Systems. *Journal of structural engineering,* 146**,** 06020003.

Foschi, R. O. 1977. Analysis of wood diaphragms and trusses. Part I: Diaphragms. *Canadian Journal of Civil Engineering,* 4**,** 345-352.

Hanaor, A. 2000. Tests of composite beams with cold-formed sections. *Journal of Constructional Steel Research,* 54**,** 245-264.
Hassanieh, A., Valipour, H. R. & Bradford, M. A. 2016a. Experimental and numerical study of steel-timber composite (STC) beams. *Journal of Constructional Steel Research,* 122**,** 367-378.
Hassanieh, A., Valipour, H. R. & Bradford, M. A. 2016b. Load-slip behaviour of steel-cross laminated timber (CLT) composite connections. *Journal of Constructional Steel Research,* 122**,** 110-121.
Hassanieh, A., Valipour, H. R. & Bradford, M. A. 2017a. Composite connections between CLT slab and steel beam: Experiments and empirical models. *Journal of Constructional Steel Research,* 138**,** 823-836.
Hassanieh, A., Valipour, H. R., Bradford, M. A. & Sandhaas, C. 2017b. Modelling of steel-timber composite connections: Validation of finite element model and parametric study. *Engineering Structures,* 138**,** 35-49.
Kalkert, R. E. & Dolan, J. D. 1997. Behavior of 8-D nailed stud-to-sheathing connections. *Forest Products Journal,* 47**,** 95-102.
Karki, D. & Far, H. 2021. State of the art on composite cold-formed steel flooring systems. *Steel Construction*.
Karki, D., Far, H. & Saleh, A. 2021. Numerical Studies into Factors Affecting Structural Behaviour of Composite Cold-Formed Steel and Timber Flooring Systems. *Journal of Building Engineering***,** 102692.
Khorsandnia, N., Valipour, H., Schänzlin, J. & Crews, K. 2016. Experimental Investigations of Deconstructable Timber-Concrete Composite Beams. *Journal of structural engineering,* 142**,** 04016130.
Kyvelou, P., Gardner, L. & Nethercot, D. A. 2017. Testing and Analysis of Composite Cold-Formed Steel and Wood−Based Flooring Systems. *Journal of Structural Engineering,* 143.
Kyvelou, P., Gardner, L. & Nethercot, D. A. 2018. Finite element modelling of composite cold-formed steel flooring systems. *Engineering Structures,* 158**,** 28-42.
Lakkavalli, B. S. & Liu, Y. 2006. Experimental study of composite cold-formed steel C-section floor joists. *Journal of Constructional Steel Research,* 62**,** 995-1006.
Li, Y., Shen, H., Shan, W. & Han, T. 2012. Flexural behavior of lightweight bamboo–steel composite slabs. *Thin-Walled Structures,* 53**,** 83-90.
Loss, C. & Davison, B. 2017. Innovative composite steel-timber floors with prefabricated modular components. *Engineering Structures,* 132**,** 695-713.
Lukaszewska, E., Fragiacomo, M. & Johnsson, H. 2010. Laboratory Tests and Numerical Analyses of Prefabricated Timber-Concrete Composite Floors. *Journal of structural engineering,* 136**,** 46-55.
Mirza, O. & Uy, B. 2009. Behaviour of headed stud shear connectors for composite steel–concrete beams at elevated temperatures. *Journal of Constructional Steel Research,* 65**,** 662-674.
Navaratnam, S., Ngo, T., Gunawardena, T. & Henderson, D. 2019. Performance Review of Prefabricated Building Systems and Future Research in Australia. 9**,** 38.
Navaratnam, S., Widdowfield Small, D., Gatheeshgar, P., Poologanathan, K., Thamboo, J., Higgins, C. & Mendis, P. 2021. Development of cross laminated timber-cold-formed

steel composite beam for floor system to sustainable modular building construction. *Structures,* 32**,** 681-690.
Originpro 2021. OriginPro-Graphing and Analysis Tool, Version number 2021. OriginLab Corporation, Northampton, MA, USA.
Parnell, R., Davies, B. W. & Xu, L. 2010. Vibration Performance of Lightweight Cold-Formed Steel Floors. *Journal of structural engineering,* 136**,** 645-653.
Rackham, J. W., Couchman, G. H. & Hicks, S. J. 2009. Composite slabs and beams using steel decking: Best practice for design and construction. *MCRMA Technical paper No.13.* Steel Construction Institute.
Standard Australia 1996. AS1393:1996 Coach screws-Metric series with ISO hexagon heads. SAI Global.
Standard Australia 2000. AS1110.1-2000 ISO Metric hexagon bolts and screws. SAI Global.
Standard Australia 2002. AS3566.1-2002; Self-drilling screws for buidling and construction industries-Part 1. SAI Global.
Standard Australia 2007. AS 1391-2007 Metallic materials -Tensile testing at ambient temperature. Standard Australia: SAI Global.
Standard Australia 2012. AS/NZS 2269.1:2012 Plywood-Structural, Part 1: Determination of structural properties-Test methods. Australia: SAI Global.
Vella, N., Gardner, L. & Buhagiar, S. 2020. Experimental analysis of cold-formed steel-to-timber connections with inclined screws. *Structures,* 24**,** 890-904.
Xu, L. & Tangorra, F. M. 2007. Experimental investigation of lightweight residential floors supported by cold-formed steel C-shape joists. *Journal of Constructional Steel Research,* 63**,** 422-435.
Yang, R., Li, H., Lorenzo, R., Ashraf, M., Sun, Y. & Yuan, Q. 2020. Mechanical behaviour of steel timber composite shear connections. *Construction and Building Materials,* 258**,** 119605.
Zhou, X., Shi, Y., Xu, L., Yao, X. & Wang, W. 2019. A simplified method to evaluate the flexural capacity of lightweight cold-formed steel floor system with oriented strand board subfloor. *Thin-Walled Structures,* 134**,** 40-51.